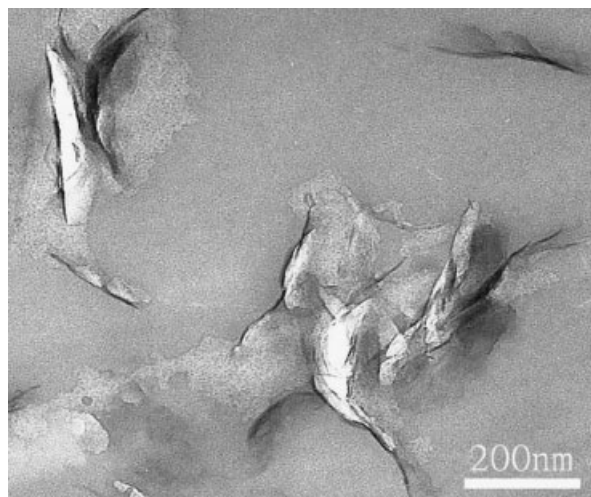


Effect of an Organically Modified Nanoclay on Low-Surface-Energy Materials of Polybenzoxazine

Huei-Kuan Fu, Chih-Feng Huang, Shiao-Wei Kuo,* Han-Ching Lin, Ding-Ru Yei, Feng-Chih Chang*

Novel low surface free energy materials of polybenzoxazine/organically modified silicate nanocomposites have been prepared and characterized. The CPC (cetylpyridinium chloride)/clay10%/poly(3-phenyl-3,4-dihydro-2H-1,3-benzoxazine) (PP-a) material possesses an extremely low surface free energy ($12.7 \text{ mJ} \cdot \text{m}^{-2}$) after 4 h curing at 200°C , which is even lower than that of poly(tetrafluoroethylene) ($22.0 \text{ mJ} \cdot \text{m}^{-2}$) calculated on the basis of the three-liquid geometric method. X-Ray photoelectron spectroscopy (XPS) shows a higher silicon content on the surface of the nanocomposites than for an average composition, which implies that the clay is more preferentially enriched on the outermost layer. In addition, the glass transition temperature (T_g) of the polybenzoxazine (PP-a) in the nanocomposite is 22.6°C higher and its thermal decomposition temperature is also 31.5°C higher than the pure PP-a. This finding provides a simple way to prepare low surface energy and high thermal stability materials.



Introduction

Materials with a low surface energy have attracted considerable attention recently because of numerous practical applications. Both poly(tetrafluoroethylene) (PTFE) and poly(dimethylsiloxane) (PDMS) are well-known materials that possess low surface free energies.^[1–4] PTFE may be regarded as the benchmark lower surface free energy material, displaying water repellency^[5] in combination with other desirable properties.^[6] However, PTFE and many fluorinated polymers have some application limitations such as high cost and poor processability.

Hybrid organic–inorganic materials have shown superior physical properties compared to conventional materials.^[7–9] Montmorillonite (MMT) clay consists of two fused

H.-K. Fu, C.-F. Huang, D.-R. Yei, F.-C. Chang
Institute of Applied Chemistry, National Chiao-Tung University,
Hsin-Chu, Taiwan (ROC)
Fax: 886-3-5131512; E-mail: changfc@mail.nctu.edu.tw
S.-W. Kuo
Department of Materials Science and Optoelectronic Engineering,
Center for Nanoscience and Nanotechnology, National Sun Yat-
Sen University, Kaohsiung, Taiwan (ROC)
Fax: 886-7-5254099; E-mail: kuosw@faculty.nsysu.edu.tw
H.-C. Lin
National Nano Device Laboratories, Hsin-Chu, Taiwan (ROC)

silica tetrahedral sheets that sandwich an edge-shared octahedral sheet of either magnesium or aluminum hydroxide. The clay can be functionalized by various organic cations through ion exchange where the metal ions are replaced by organic cations that intercalate the silicate layers to make the clay organophilic and compatible with polymers.^[10,11]

Polybenzoxazines have been developed as a new type of phenolic resin and have attracted great interest from academia and industry because of their fascinating characteristics, such as low water absorption, high moduli,^[12] high glass-transition temperature,^[13–15] and low surface free energy.^[16,17] In this study, a cetylpyridinium chloride (CPC)-modified clay is employed to prepare polybenzoxazine (PP-a)/clay nanocomposites. The detail morphologies, intermolecular and intramolecular interactions, and thermal and surface properties of PP-a/clay nanocomposites are investigated in this study.

Experimental Part

Preparation of CPC-Modified Clays

Na⁺ MMT (0.3 g) was dispersed in 1 L of deionized water and stirred continuously at 80 °C for 4 h. The CPC (0.156 g) was placed into another flask, and 10% hydrochloric acid (1 mL) and ethanol (5 mL) were added and then stirred at 80 °C for 1 h. The intercalating agent solution was then poured into the clay suspension solution and stirred vigorously at 80 °C for 4 h. The resulting white precipitate was separated by filtration and then washed several times with warm deionized water. The final product was dried in a vacuum oven at 65 °C overnight.

Preparation of CPC/Clay/PP-a Nanocomposites by a Solvent Method

The organically modified MMT (3 g) was dispersed homogeneously in tetrahydrofuran (THF, 10 mL) and stirred at room temperature for 2 h. The P-a monomer was added into the organically modified clay suspension and vigorously stirred at room temperature for 48 h. The solution was spin-coated onto a glass slide (100 × 100 × 1 mm³) operating at 300 rpm for 45 s. The sample was left to dry at 65 °C and then cured in an oven at 200 °C for 4 h.

Characterization

Thermal analyses were performed using a Du-Pont (DSC-2010). The sample was preheated at a scan rate of 20 °C · min⁻¹ from 30 to 150 °C under a nitrogen atmosphere. The sample was quickly cooled to 10 °C from the first scan and then scanned between 30 and 250 °C at the scan rate of 20 °C · min⁻¹. Thermal stabilities of the cured nanocomposites were investigated using a TA Instruments Q50 apparatus at a heating rate of 20 °C · min⁻¹ from 30 to 800 °C. Wide-angle X-ray diffraction (WAXD) experiments were

carried on a Rigaku D/max-2500 type X-ray diffraction instrument with Cu K_α radiation ($\lambda = 1.54 \text{ \AA}$) using a Ni filter. Data were recorded in the range of $2\theta = 1$ to 20 at a scanning rate of 0.6 deg · min⁻¹. Transmission electron microscopy (TEM) images were obtained on a Hitachi H-7500 operating at 100 kV using a sample with a thin-section of $\approx 70 \text{ nm}$. For contact angle measurements, deionized water, ethylene glycol, and diiodomethane were used as standards to measure the surface free energies. The advancing contact angle measurement of a sample was determined at 25 °C after injection of a liquid drop (5 μL) onto the surface and a Krüss GH-100 goniometer interfaced to image-capture software was employed to perform the measurement. X-Ray photoelectron spectroscopy (XPS) characterization was performed using a VG Microlab 310F Spectrometer equipped with an Al K_α X-ray source (1486.6 eV). Surface roughness profiles and phase imaging of the film structure were acquired using a digital Instruments DI5000 scanning probe microscope in the tapping mode with a typical radius of curvature <7 nm.

Results and Discussion

Figure 1 shows the XRD plots for the a) pristine clay, the b) CPC-modified clay and (c,d, and e) PP-a/clay nanocomposites with various CPC-modified clay contents. The original clay has an intergallery spacing of 1.28 nm. The CPC-modified clay shows a *d* spacing of 2.56 nm, which corresponds to an increase of 1.28 nm and provides evidence that the clay galleries were expanded after CPC insertion. The modification of the hydrophilic silicate layer renders it more hydrophobic and consequently more compatible with the P-a monomer. In these PP-a/clay nanocomposites, the (001) diffraction peak of $2\theta = 2.78^\circ$ for all clay contents corresponds to a basal spacing of 3.17 nm.

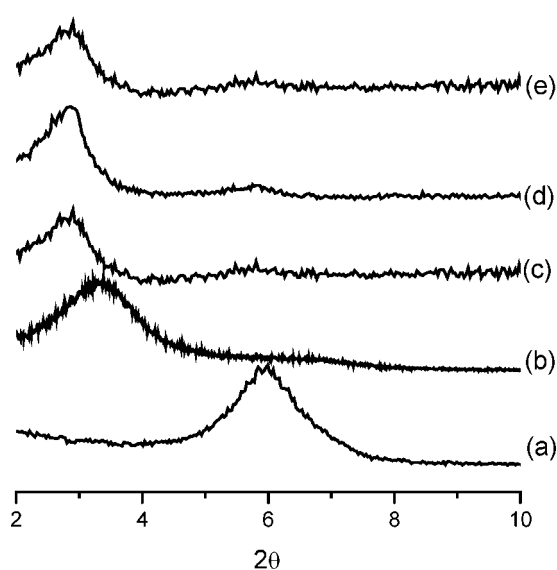


Figure 1. X-Ray diffraction patterns of a) pure clay, and b) CPC/clay, c) PP-a/clay 3 wt.-%, d) 5 wt.-%, and e) 10 wt.-%.

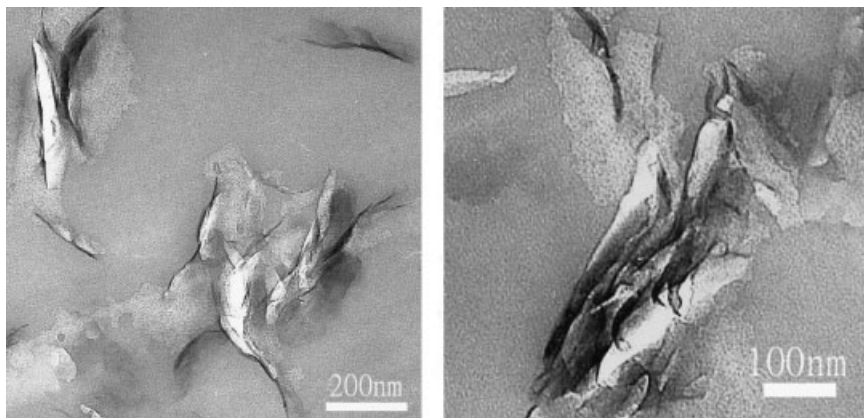


Figure 2. TEM micrographs of the PP-a nanocomposites that contain 3 wt.-% clay: (left) low magnification and (right) high magnification.

When the PP-as are inserted within the galleries of the MMT, the d spacing is increased from 1.28 for the pristine MMT to 3.17 nm for the CPC/clay/PP-a nanocomposites. Because of the angle of detection limitation of XRD, it is impossible to detect a diffraction angle below 1° . Thus, it is necessary to observe the true structure and distributions of these silica platelets by using TEM. TEM images for a CPC/clay/PP-a nanocomposite with a 3% inorganic clay loading are shown in Figure 2, which indicates the partial aggregation of these clay platelets configuration. From the XRD and TEM results, these nanocomposites all possess intercalated structures.

Table 1 presents the thermal stabilities of the CPC/clay/PP-a nanocomposites investigated by DSC and TGA analyses. The glass transition temperature of the nanocomposites increase with the increase of clay loading, which indicates that the motion of the PP-a is retarded by the silicate layers. In addition, the thermal stability of the nanocomposites is also improved, and both the thermal

degradation temperature (T_d) and the char yield of these nanocomposites are increased with the increase of the clay loading. When increasing the clay loading to 10%, the thermal degradation temperature is 357.1°C , an increase of 35.4°C in comparison to virgin PP-a. Because of the nature of the inorganic clay, the char yield of the nanocomposites increases with the increase of clay content as would be expected.

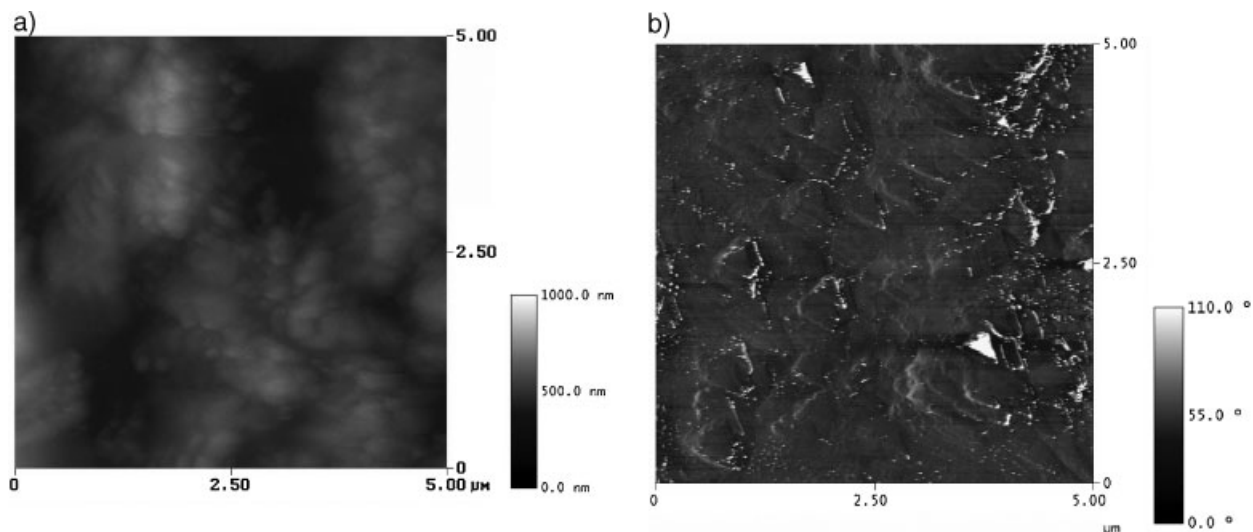
Surface free energies of PP-a/clay nanocomposites with various clay contents are summarized in Table 1 based on van Oss and Good's three-liquid method.^[18,19] The surface roughness of all specimens are less

than 50 nm, therefore, the influence of topography on the surface free energy is considered insignificant.^[20,21] It is clear that the increase of clay content results in a significant decrease in surface free energy (from 21.4 to $12.7\text{ mJ}\cdot\text{m}^{-2}$). Compared with the surface free energy of PTFE ($22\text{ mJ}\cdot\text{m}^{-2}$) determined by using the same testing liquids and method of calculation,^[22] all PP-a/clay nanocomposites give a lower surface energy than PTFE. Kadar et al.^[23] studied the surface free energy of the neat and organophilized clays, that of the uncoated layered silicates is extremely high at $257\text{ mJ}\cdot\text{m}^{-2}$, while the CPC-modified clay is drastically reduced at $32\text{ mJ}\cdot\text{m}^{-2}$. The compatibility between the intercalated agent and polymer matrix (PP-a) is very important. Phiriyawirut et al.^[24] studied the immiscibility of PP-a/clay nanocomposites and indicated that delamination of the silicate layers is strongly dependent on the compatibility between the intercalated agent and the monomer (P-a). Hence the incorporation of CPC-modified layered silicates into the

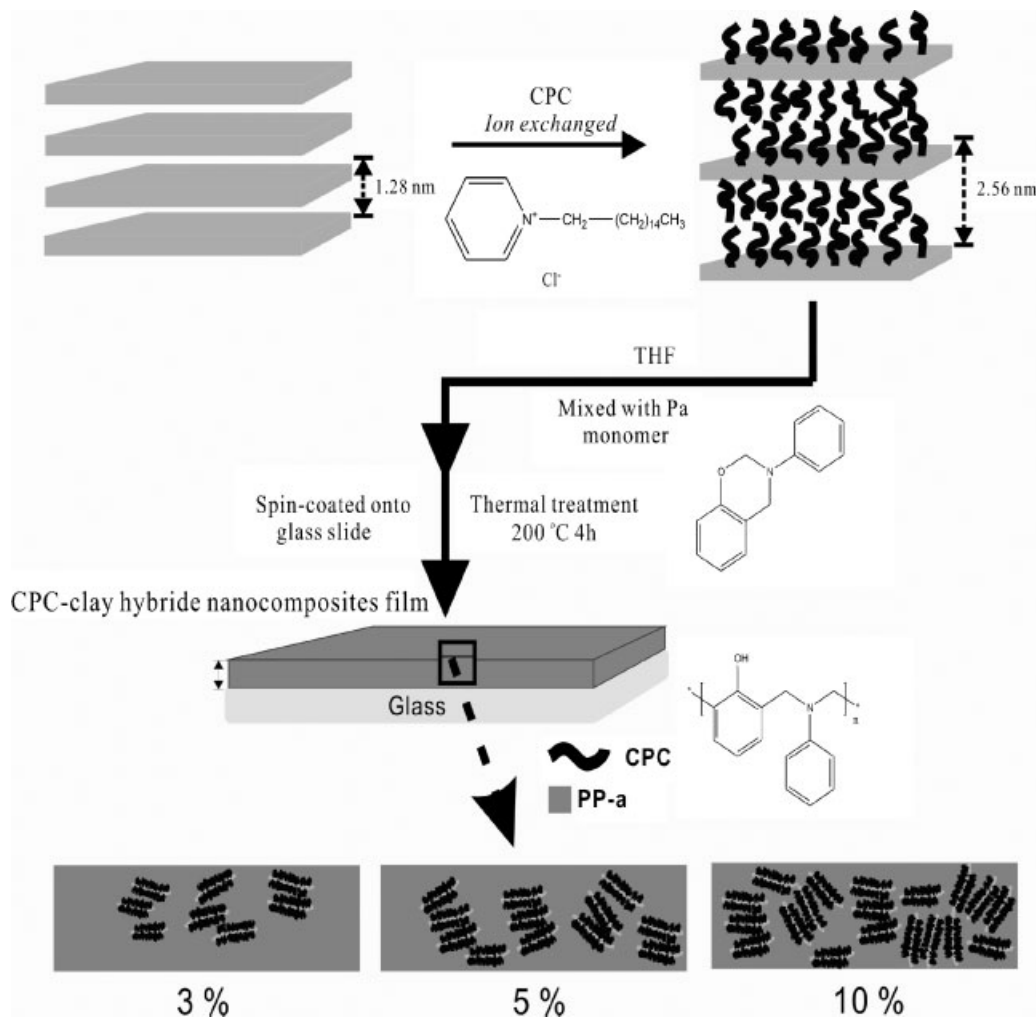
Table 1. Advancing contact angles, surface free energies, roughness, XPS analysis, and thermal properties of PP-a/clay nanocomposites.

Sample	Contact angle			γ	Roughness	XPS ^{a)}	T_g	T_d ^{b)}	Char yield (600 °C)
	deg								
	H ₂ O	DIM	EG						
PP-a	113.1	72.7	85.4	21.4	2.6	0	126.1	321.7	40.1
PP-a/3% clay	110.7	84.6	85.6	15.7	20.1	6.8	134.2	325.6	44.7
PP-a/5% clay	112.2	89.3	86.8	13.6	34.6	7.6	142.8	335.5	47.4
PP-a/10% clay	116.4	91.4	86.2	12.7	45.1	10.9	148.7	353.2	48.1

^{a)}Silicon content (mol-%); ^{b)}The decomposition temperature (T_d) of the 5% weight loss.



■ Figure 3. AFM images of CPC/clay 10%/PP-a: a) topography image and b) phase image.



■ Scheme 1. Representation of the intercalated agent that was inserted into the silicate layers via ion exchange and the preparation of PP-a nanocomposites by thermal treatment.

PP-a is able to help its dispersion within the polymer matrix (PP-a).

As a result, the low surface energy must come from the incorporation of the modified long alkyl organic clay, which leads to chemical and topographical modification of the nanocomposites' surface and enhances the hydrophobic surface property.^[25]

Figure 3(a) and 3(b) present the topography and phase image of the CPC/clay10%/PP-a nanocomposites investigated by atomic force microscopy (AFM). These results indicate that the CPC-modified clays preferably reside on the surface and the effect of the surface roughness is present but considered to be less important.

Scheme 1 displays schematic plots that show the intercalation agent inserting into the silicate layers by ion exchange, the preparation by spin coating of the CPC/clay/PP-a blending solution, and thermal treatment. Table 1 shows the atomic fraction of silicon by XPS analyses, which indicates that the CPC-modified clays preferably reside on the surface. The surface chemical structure and composition both have significant influence on the measured contact angle and resultant surface free energy of the nanocomposite. Combining our analyses of XPS and contact angle measurement, we speculate that the decrease of the surface free energy in the present case is a result of the CPC-modified clays.

Conclusion

A series of CPC/clay hybrids of polybenzoxazine (PP-a) have been prepared and their thermal properties and surface free energy have been characterized. The surface free energy of the CPC/clay/PP-a nanocomposites prepared by a simple thermal treatment is significantly reduced. The lowest surface free energy obtained of the CPC/clay10%/PP-a is 12.6 mJ^{-2} , which is even lower than that of PTFE ($22.0 \text{ mJ} \cdot \text{m}^{-2}$). In addition to decreasing the surface free energy of the nanocomposites, the thermal properties are improved after the incorporation of 10% of the organically modified montmorillonite.

Received: February 12, 2008; Revised: March 25, 2008; Accepted: April 14, 2008; DOI: 10.1002/marc.200800092

Keywords: clay; low surface free energy; nanocomposites; polybenzoxazine

- [1] S. R. Coulson, I. Woodward, J. P. S. Badyal, S. A. Brewer, C. Willis, *J. Phys. Chem. B* **2000**, *104*, 8836.
- [2] M. Jin, X. Feng, J. Xi, J. Zhai, K. Cho, L. Feng, L. Jiang, *Macromol. Rapid Commun.* **2005**, *26*, 1805.
- [3] L. Feng, Z. Zhang, Z. Mai, Y. Ma, B. Liu, L. Jiang, D. Zhu, *Angew. Chem. Int. Ed.* **2004**, *43*, 2012.
- [4] H. Hillborg, N. Tomczak, A. Olah, H. Schonherr, G. J. Vancso, *Langmuir* **2004**, *20*, 785.
- [5] S. Wu, "Polymer Interface and Adhesion", Marcel Dekker, New York 1982.
- [6] A. E. Feiring, J. F. Imbalzano, D. L. Kerbow, *Adv. Fluoroplast. Plast. Eng.* **1994**, 27.
- [7] Y. Kojima, A. Usuki, M. Kawasumi, A. Okada, T. Kurauchi, O. Kamigaito, *J. Polym. Sci., Part A: Polym. Chem.* **1993**, *31*, 1755.
- [8] D. R. Yei, S. W. Kuo, H. K. Fu, F. C. Chang, *Polymer* **2005**, *46*, 741.
- [9] X. Fu, S. Qutubuddin, *Polymer* **2001**, *42*, 807.
- [10] X. Huang, W. J. Brittain, *Macromolecules* **2001**, *34*, 3255.
- [11] F. L. Beyer, N. C. B. Tan, A. Dasgupta, M. E. Galvin, *Chem. Mater.* **2002**, *14*, 2983.
- [12] H. Ishida, D. J. Allen, *J. Polym. Sci., Part B: Polym. Phys.* **1996**, *34*, 1019.
- [13] H. Ishida, Y. Rodriguez, *Polymer* **1995**, *36*, 3151.
- [14] Y. J. Lee, S. W. Kuo, Y. C. Su, J. K. Chen, C. W. Tu, F. C. Chang, *Polymer* **2004**, *45*, 6321.
- [15] Y. C. Su, S. W. Kuo, D. R. Yei, H. Xu, F. C. Chang, *Polymer* **2003**, *44*, 2187.
- [16] C. F. Wang, Y. C. Su, S. W. Kuo, C. F. Huang, Y. C. Sheen, F. C. Chang, *Angew. Chem. Int. Ed.* **2006**, *45*, 2248.
- [17] C. F. Wang, Y. T. Wang, P. H. Tung, S. W. Kuo, C. H. Lin, F. C. Chang, *Langmuir* **2006**, *22*, 8289.
- [18] C. J. van Oss, L. Ju, M. K. Chaudhury, R. J. Good, *J. Colloid Interface Sci.* **1989**, *128*, 313.
- [19] C. J. van Oss, L. Ju, M. K. Chaudhury, R. J. Good, *Chem. Rev.* **1988**, *88*, 927.
- [20] J. Drelich, J. D. Miller, R. J. Good, *J. Colloid Interface Sci.* **1996**, *179*, 37.
- [21] R. J. Good, C. J. van Oss, "Modern Approaches to Wettability: Theory and Applications", M. E. Schrader, G. Loeb, Eds., Plenum Press, New York 1992, pp. 1–27.
- [22] U. Yoshimasa, N. Takashi, *Langmuir* **2005**, *21*, 2614.
- [23] F. Kadar, L. Szazdi, E. Fekete, B. Pukanszky, *Langmuir* **2006**, *22*, 7848.
- [24] P. Phiriyawirut, R. Magaraphan, H. Ishida, *Mater. Res. Innovat.* **2001**, *4*, 187.
- [25] J. J. Lin, C. C. Chu, M. L. Chiang, W. C. Tsia, *Adv. Mater.* **2006**, *18*, 3248.